IJPSR (2024), Volume 15, Issue 5 **(Research Article)**

INTERNATIONAL JOURNAL OF PHARMACEUTICAL SCIENCES AND RESEARCH

Received on 22 October 2023; received in revised form, 10 January 2024; accepted, 28 February 2024; published 01 May 2024

CHARACTERIZING MICROSTRUCTURES AND CRYSTALLOGRAPHIC PHASES IN KIDNEY STONES FROM THE NAGPUR REGION, MAHARASHTRA

Apurva S. Wase, Sudipta Sarkar and Mashitha Pise *

Department of Biochemistry, Hislop College, Temple Road, Nagpur - 440001, Maharashtra, India.

Keywords:

X-Ray diffraction, Urolithiasis, Microstructures, Crystallographic Phases, Quantitative analysis

Correspondence to Author:
Dr. MashithaPise, Ph.D.,

Assistant Professor, HoD,
Department of Biochemistry,
Hislop College, Temple Road, Nagpur - 440001, Maharashtra, India.

E-mail: pmmashi@gmail.com

ABSTRACT: The increasing incidence of urolithiasis in the Asian population has been noted, and this condition can result in renal failure. The recurrent nature of stone formation evokes significant concern, as it leads to repetitive episodes of calculi development, ultimately resulting in gradual renal deterioration. Consequently, there exists a pressing imperative for comprehending the composition and etiological factors contributing to nephrolithiasis. A total of 14 kidney stone samples obtained from patients were subjected to X-ray diffraction (XRD), Fourier transform infrared spectroscopy (FT-IR), and Scanning electron microscopy (SEM) analysis. XRD analysis using MATCH software was employed to determine the crystallographic phases and quantitative abundances of different minerals. SEM examination was conducted to observe the microstructures of the kidney stones. Phase estimate findings showed that whewellite was the sole phase present in the kidney stone samples KS4, KS5, KS8, KS9, KS11, and KS12. struvite and hydroxyapatite were present in KS1, KS2, and KS13. Moreover, the study of KS3, KS6, and KS7 revealed varied levels of struvite, hydroxyapatite, and Weddellite. These microstructural features, investigated using the SEM and FTIR methods, revealed striking microstructural differences which vary with the type of stone. This study provides insights into the composition and microstructure of kidney stones in patients from the Nagpur District. The analysis revealed a higher prevalence of oxalates, struvite, and mixed groups in the kidney stones of the population. These findings contribute to a better understanding of kidney stone formation and may aid in developing preventive and management strategies for urolithiasis in the region.

INTRODUCTION: The composition of kidney stones can be classified into two parts: an organic matrix containing mainly proteins, lipids, carbohydrates, and cellular components, and biominerals. Calcium oxalate monohydrate or whewellite is by far the most frequent mineral type in human kidney stones [1].

QUICK RESPONSE CODE

DOI: 10.13040/IJPSR.0975-8232.15(5).1433-40

This article can be accessed online on www.ijpsr.com

DOI link: https://doi.org/10.13040/IJPSR.0975-8232.15(5).1433-40

The etiology of whewellite stones tends to be unclear. In conditions like hyperoxaluria and hypercalciuria, elevated amounts of calcium and oxalate in urine are linked to their development. However, the genesis is multifactorial; metabolic, dietary, or genetic conditions can be attributed to it [2].

Although kidney stones are removed by either surgical or non-invasive clinical procedures, the increasing frequency of recurrence is a significant concern, calling for a thorough investigation of the composition and quantification of kidney stone disease [3]. Analytical methods such as Scanning Electron Microscopy (SEM), Fourier transform

infrared (FT-IR) spectroscopy, and X-ray powder diffraction (XRD) are used for qualitative and quantitative classification of kidney stones [4, 5]. A clinical study was conducted to investigate the role of mineral phases in kidney stone pathogenesis, likely confounded by an unknown variety of underlying renal pathologies. Therefore, we propose to examine the microstructure and morphology of kidney stones in patient populations that have been carefully phenotyped relative to renal stone etiology.

Moreover, the goal is to find analytical techniques to accurately determine stone composition and visualize the mechanism of nucleation. Knowledge of the quantitative mineralogy of kidney stones is important for ascertaining their etiology and further developing prophylactic.

MATERIALS AND METHODS:

Sample Preparation: A total of 14 kidney stones were collected, extracted surgically, or expelled from the patients' bodies. Patient donors hospitalized at Vasant Holium Laser Endo-Urology & Andrology Clinic and Ketki Nursing Home in Nagpur, from March 2021 to January 2022, were involved in the study. General information about the patients was gathered through a questionnaire aimed at collecting socio-demographic status, medical history, and complaints. All samples were collected in sterilized wide-mouthed containers. The stones underwent surface sterilization with distilled water to remove body fluids and blood clots. Subsequently, they were dried at room temperature for 24 hours and stored in pre-cleaned glass vials at 4°C in refrigerators.

X-ray Diffraction Studies: The XRD measurements were conducted using a Rigaku MiniFlex diffractometer with a CuKα tube operating at λ= 1.54056 Å. The XRD patterns were recorded within the Bragg's angles range of $10° < 2\theta < 90°$ at room temperature, with operational parameters set at a tube voltage of 40 kV and a tube current of 40 mA. Manual identification of XRD patterns is cumbersome; therefore, computational tools were employed to identify the phases [6].

We utilized the 'Crystal Match!' software, integrated with the Crystallography Open Database, to identify the peaks associated with different phases.

SEM Analysis: For SEM analysis, the kidney stones were washed, air-dried, and mounted on aluminum stubs using carbon tape. Subsequently, a thin layer of gold was applied to the samples for improved visualization. The samples were observed under a scanning electron microscope (JEOL-JSM-840, Japan), and images were captured at 10 kV using the secondary electron detector (LEI).

FT-IR Analysis: FT-IR analysis was performed using a Shimadzu IRAffinity-1 equipment. The spectra were obtained via the diffuse reflectance mode in the range of 400-4000 cm^{-1}. Two milligrams of sample were weighed with 198 mg of KBr and measured with a resolution of 2 cm^{-1} using 100 scans.

RESULTS:

Quantitative Phase Analysis: All sample stones represented six mineral types: calcium oxalate monohydrate, oxalate monohydrate-calcium oxalate dihydrate, struvite-hydroxyapatite, calcium oxalate dihydrate-struvite, calcium oxalate monohydrate-struvite, and calcium oxalate monohydrate-hydroxyapatite.

The peak profiles were fitted with pseudo-Voigt functions with asymmetry correction at low angles, as shown in **Fig. 1**. The results of the XRD diffraction of samples KS1–KS14, along with the patients details **Table 1**.

The structural parameters (a, b, c, and β) in Table 2 for KS1–KS14 do not differ significantly from the values reported in the literature for single-crystal studies of whewellite, weddellite, and hydroxyapatite.

The quantitative estimation of individual phases, showed that the kidney stone samples KS4, KS5, KS8, KS9, KS11, and KS12 were monophasic; i.e., whewellite was the only available phase. On the other hand, KS1, KS2, and KS13 indicated the presence of struvite (51-97 wt. %) and hydroxyapatite (2-48 wt. %), while KS10 had both as major phases (51.4-48.6 wt. %).

The quantitative phase analysis of KS3, KS6, and KS7 showed varying amounts of struvite (3.4 wt. %), hydroxyapatite (28.3 wt.%), and Weddellite (37.1 wt.%) phase along with the whewellite (62-96 wt.%) phase as the major phase **Table 2**.

TABLE 1: PHASE COMPOSITION AND QUALITATIVE PARAMETERS OF SAMPLES KS1-KS14

Sample	Gender	Age	Stone Size	Mineral Composition %				2Θ(theta)	FWHM
				COM	COD	STR	HAP		
KS1	Male	28	7	-	97.2	2.8	-	14.95	0.0839
KS2	Female	23	10	-	-	75.8	24.2	26.80	0.1259
KS3	Male	28	11	96.6	-	3.4	-	14.89	0.1600
KS4	Male	70	7	100	-	-	-	14.94	0.1600
KS5	Male	63	8	100	-	-	-	15.02	0.1600
KS6	Male	36	8	62.9	37.1	-	-	30.07	0.1200
KS7	Male	64	7	71.7	-	-	28.3	14.92	0.1600
KS8	Female	58	6	100	-	-	-	15.02	0.3200
KS9	Male	21	4	100	-	-	-	15.02	0.1600
KS10	Male	43	6	-		51.4	48.6	31.8	0.2400
KS11	Male	28	8	100	-	-	-	24.4	0.2400
KS12	Male	63	3	100	-	-	-	24.42	0.2400
KS13	Male	50	6	-	-	91.2	8.8	14.96	0.2400
KS14	Male	45	3	-	26	17	57.3	32.5	0.1200

FT-IR Characterization: A broad absorption peak observed between 3585 to 2767 cm^{-1} is attributable to symmetric and asymmetric stretching vibration of hydrogen bond (O-H) of water and the N-H in the $NH4^{+}$ group **Fig. 2A**. The symmetric bending vibration and unsymmetrical bending vibration of the N–H ($NH4^{+}$) were observed at peaks of 1541.70 and 1417.67 cm^{-1}. A very weak peak at 1471 cm^{-1} is due to HNH deformation of $NH4^{+}$, indicating the presence of struvite. Peaks at the region at 1649 and 1317 cm^{-1} stretching of oxalate anion showing that the sample contains Weddellite [7]. Bands at 777, 669, and 514 cm^{-1} were assigned to vibrations of the O–C–O group in weddellite. The medium band cantered at 1031 and 1139 cm^{-1} shows v3 stretching vibrations due to phosphate of hydroxyapatite. Hence the FT-IR spectrum shows the sample to be a mixture of calcium oxalate dihydrate and struvite.

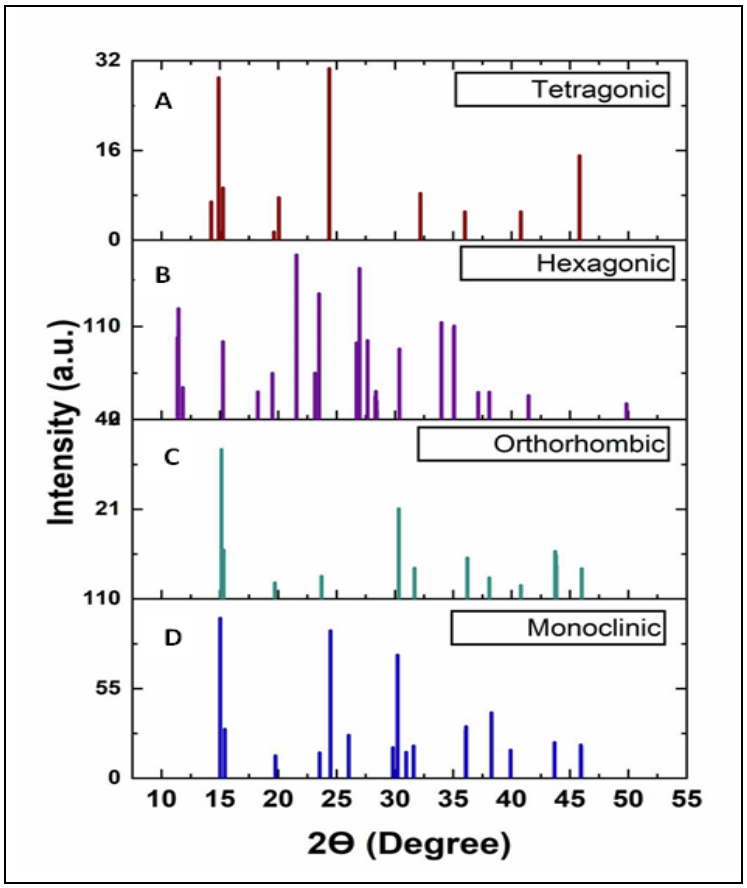

FIG. 1: DIFFRACTION PATTERN OF KIDNEY STONES A) KS1, B) KS2 C) KS3 D) KS5

Fourier transform infrared spectrum of the stone sample **Fig. 2B** shows a strong peak of the sample at 3500 and 2358 cm^{-1}, which are due to OH stretching vibration of crystallized water. An intense absorption band at 2806 cm^{-1} and 2358 cm^{-1} shows intermolecular hydrogen-bonded OH stretch. Peaks at the region at 1680 and 1309 cm^{-1} were attributed to symmetric and asymmetric stretching of oxalate anion showing that the sample contains whewellite. The sharp peaks at 781 cm-1 are due to O–C=O, and the wideband at 615 cm^{-1} and 522 cm^{-1} can be assigned to the bending modes of the water molecule.

SEM Morphology: The SEM analysis is used to study crystal structures and chemical compositions in diverse kidney stones, revealing significant morphological and compositional variations. Monoclinic whewellite stones displayed plank-like, brick-like arrangements **Fig. 3A-B**, with crystals exhibiting a regular or staggered arrangement that was relatively tight and orderly. Calcium oxalate deposits appeared as dense aggregates of elongated calcified strands, showing a banded pattern indicative of calcified collagen fibres, mixed with aggregated spherulitic units. The surfaces of the laminations in KS7 **Fig. 3C** displayed a combination of smooth textures, diverse-shaped protrusions, and craters or pores of different sizes. Irregular deposits of hydroxyapatite between the laminae were observed. The shape and microstructure of mixed stones varied with distinct components. For example, calcium oxalate-struvite mixed stones, as shown in **Fig. 3E**, showed that the basic unit of the structure was lamination made up of crystals with coarse surfaces filled with fine spherules aggregated over them [8].

The fine concentric laminations composed of struvite formed the framework, whereas the deposition of hydroxyapatite occurred as amorphous fine granules between struvite crystals or surrounded struvite crystals **Fig. 3F**. Localized differences in the crystalline or amorphous contents could be seen, but the overall composition was the same. The presence of massive spherulites with sharp rhombic crystals was induced by the high concentration of mucoprotein and inflammatory debris from the urine [9]. The concentration of mucoprotein could be due to an unbalanced diet. Weddellite stones displayed agglomerates of rhomboidal planes aggregated together with octahedral-shaped crystals **Fig. 3G-H**.

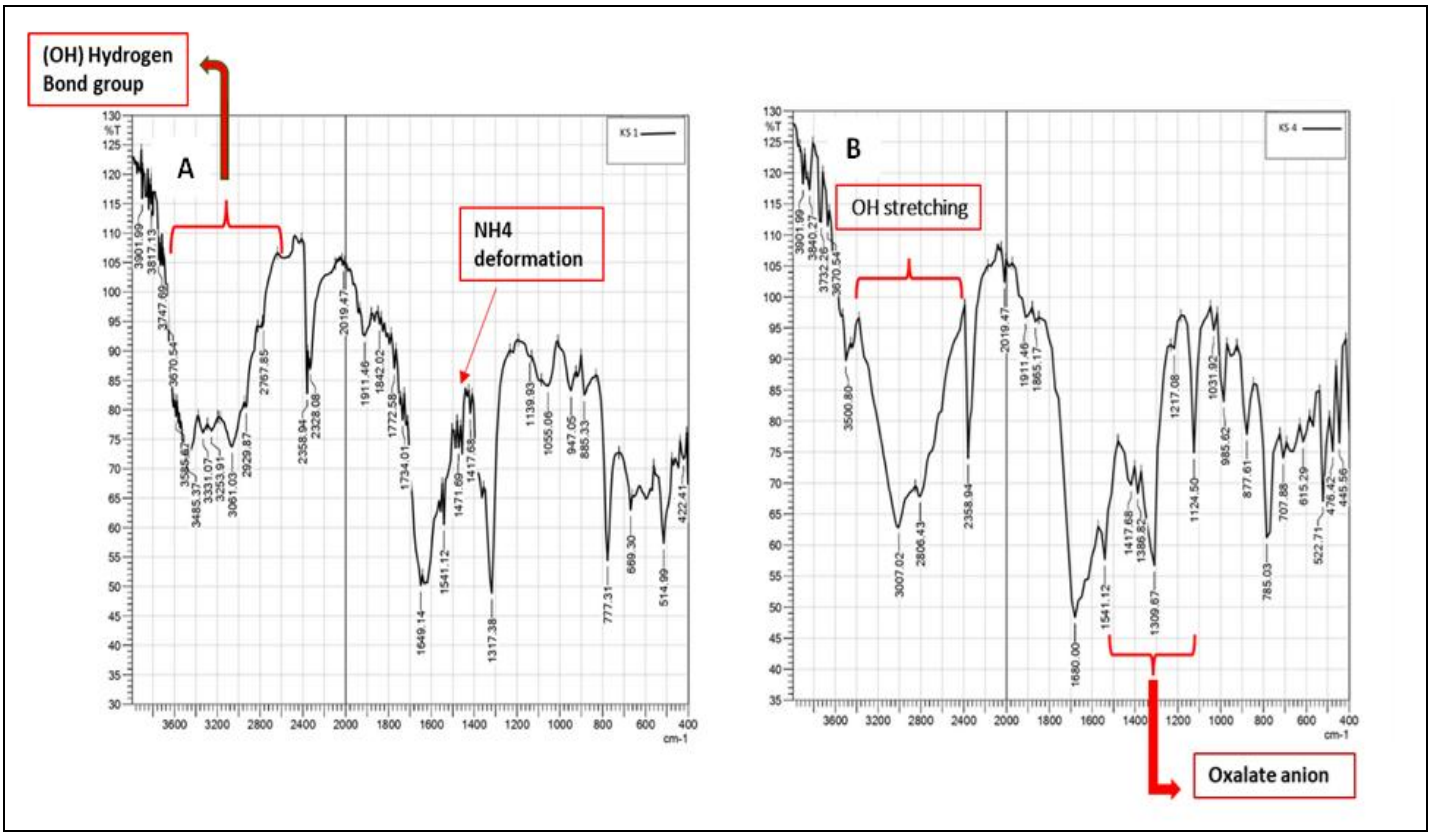

FIG. 2: FT-IR SPECTRA A) KS1 struvite & WEDDELLITE (COD), B) KS4 WHEWELLITE (COM)

Sample KS14 **Fig. 3F** images showed that the hydroxyapatite stones exhibited a range of surface features and textures. The stones displayed a porous structure with irregularly shaped crystals and mineralized deposits. The surface morphology of the stones exhibited both smooth and rough surface areas, indicating variations in crystal growth and mineralization patterns. KS14 **Fig. 3D** is seen to have peculiar globular structures encountered with a much smaller size, which is 200 nm. This can be presumed as nanobacteria, as the SEM details match with earlier reports [10, 11]. SEM findings demonstrated a resemblance in size and morphology between the observed nanobacteria and those documented in previous studies. Studies conducted earlier have reported the occurrence of nanobacteria in 97% of kidney stones, along with its presence in other diseases like atherosclerosis [12, 13].

TABLE 2: STRUCTURAL PARAMETERS OF CONSTITUENT PHASES OF KIDNEY STONES

S. no.	Phase	Crystal System	Space Group	Unit-Cell dimensions				Crystalline size/nm
				a/Å	b/Å	c/Å	β/°	
KS1	struvite	Orthorhombic	Pmn21	6.9550	6.1420	11.2180	-	849
	Weddellite	Tetragonal		12.371		7.3540		
KS2	struvite	Orthorhombic	Pmn21	6.9550	6.1420	11.2180	-	398.5
	Hydroxyapatite	Hexagonal	P 63/m	9.4210		6.8800		
KS3	Whewellite	Monoclinic	P1 21/a 1	6.2900	14.5830	10.1160	109.46	304.7
	struvite	Orthorhombic	Pmn21	6.9500	6.1420	11.2180		
KS4	Whewellite	Monoclinic	P1 21/a 1	6.2900	14.5830	10.1160	109.46	445
KS5	Whewellite	Monoclinic	P1 21/a 1	6.2900	14.5830	10.1160	109.46	445.2
KS6	Whewellite	Monoclinic	P1 21/a 1	6.2900	14.5830	10.1160	109.460-	445
	Weddellite	Tetragonal	1 4/m	12.37		7.3550		
KS7	Whewellite	Monoclinic	P1 21/a 1	6.2900	14.5830	10.1160	109.460	445.2
	Hydroxyapatite	Hexagonal	P 63/m	9.4210		6.8800		
KS8	Whewellite	Monoclinic	P1 21/c 1	6.2900	14.5830	10.1160	109.46	222.6
KS9	Whewellite	Monoclinic	P1 21/a 1	6.2900	14.5830	10.1160	109.46	-
KS10	struvite	Orthorhombic	Pmn21	6.9550	6.1420	11.2180	107.9	727
	Hydroxyapatite	Hexagonal	P 63/m	9.4210		6.8800		
KS11	Whewellite	Monoclinic	P1 21/a 1	6.2900	14.5830	10.1160	109.46	301
KS12	Whewellite	Monoclinic	P1 21/c 1	6.2900	14.5830	10.1160	109.46	301
KS13	struvite	Orthorhombic	Pmn21	6.9550	6.1420	11.2180	107.9	727
	Hydroxyapatite	Hexagonal	P 63/m	9.4210		6.8800		
KS14	Hydroxyapatite	Hexagonal	P 63/m	9.4210		6.8800		476
	Weddellite	Tetragonal	1 4/m	12.37		7.3550		

DISCUSSION: The current study was conducted to analyse the microstructural and mineralogical study of kidney stones from the Nagpur region of Maharashtra. Analytical techniques such as X-ray Diffraction, Scanning Electron Microscopy, and FT-IR spectroscopy were utilized, and it was found that all techniques revealed important insights regarding the stone's microstructural details. Multiple factors can be responsible for the nucleation process, such as Randall's Plaque on the surface of the papilla, whewellite coating on the plate, or the crystallization of urine particles. After nucleation, consecutive precipitation of urine-forming minerals leads to aggregation. Previous studies from other countries, such as Italy, Iran, and Sri Lanka, have consistently reported whewellite and Weddellite as the most commonly found phases in kidney stone mineralogy [14]. Investigations on stone samples from the Nagpur region, Maharashtra, align with these findings. However, we have also observed higher occurrences of struvite (35%) and struvite-Hydroxyapatite stones [15–17]. As bacterial infections play a significant role in the formation of struvite stones, therefore this can be related to the increasing frequency of urinary tract infection (UTIs) cases in the population of India as reported in recent years [18, 19]. In SEM analysis, one of specimens exhibited aggregations comprising bacteria with spherical or ovoid morphology, measuring approximately 200 nanometres in diameter. Based on these observations, it is plausible to classify these entities as nanobacteria **Fig. 3D.** The association between nanobacteria and urolithiasis has been well-established in previous studies. Nanobacteria are cytotoxic, atypical gram-

negative bacteria that accumulate in the kidneys and subsequently in the urine. The presence of nanobacteria in kidney stones indicates that the organisms may be involved in kidney stone formation.

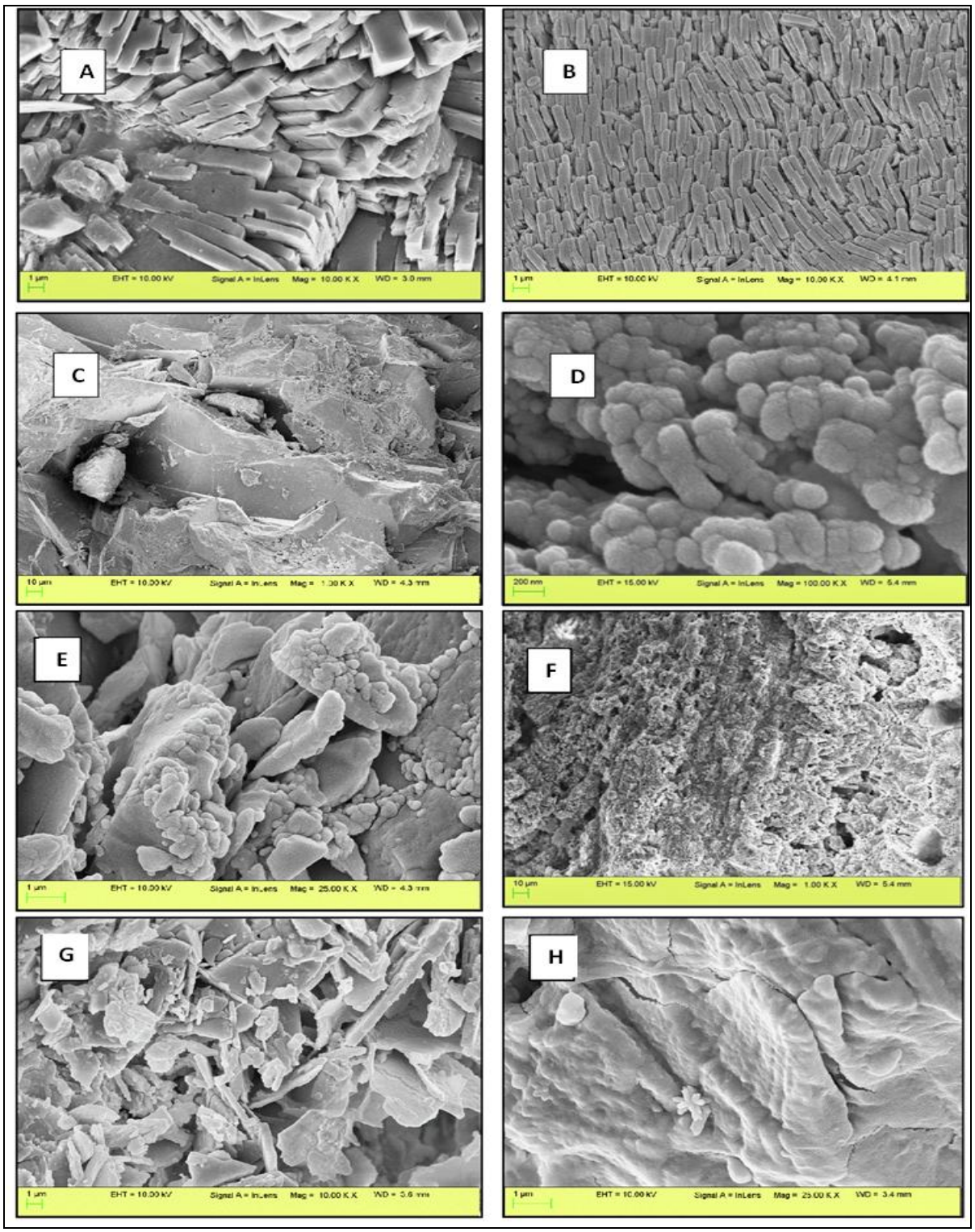

FIG. 3: SEM IMAGES OF KIDNEY STONES TO OBSERVE THEIR MORPHOLOGY. A) MONOCLINIC WHEWELLITE WITH ORDERLY LAYERED PLANES OF KS4, B) RECTANGULAR PLATES OF KS8, C) POROUS STRUCTURE OF HAP IN KS7, D) A SMALL SIZENANOBACTERIA, (SCALE BAR 200 NM) IN KS14, E) AGGREGATES OF STRUVITE IN KS2, F) RHOMBOIDAL PLANE OF WEDDELLITE AND SPHERULITES CRYSTALS OF STRUVITE OF KS14 G) MIXTURE OF HAPHAZARD PLATES OF COD AND STRUVITE CRYSTAL ACCUMULATION IN KS1, H) TETRAGONAL WEDDELLITE OBSERVED BY A BIPYRAMIDAL-PRISMATIC CRYSTAL OF KS6

However, many studies support the theory that nanobacteria act as a nidus for stone formation, as they are capable of accumulating apatite in the kidney. Nanobacteria attach themselves to the surface of the culture vessel, subsequently forming apatite structures resembling caves. These structures vary in terms of stone types, weights, and cultural positivity and are characterized by tresses and a concave surface [10, 20]. Based on SEM analysis, a few of samples exhibited characteristics consistent with hydroxyapatite **Fig. 3F.** Presence of radial, compact concentric organization seen emerging from the centre is suggestive of a mesoscopic pattern found in hydroxyapatite stones morphology. Major causes identified for the formation of such microstructural features are accorded to dietary disorders like severe Hyperoxaluria, low diuresis and/or high oxalate-rich food consumption or a low fluid intake. This sort of stone is becoming more and more prevalent in Maharashtra [19, 21]. At high concentrations of Mg^{2+}, there is a decreased calcium oxalate crystallization and growth which makes stone porous [22]. It is clear from the elemental composition in the stone matrix that different mineral compositions may be included depending on chemical interactions, pH variations, and urine supersaturation. The purity and shape of crystals are also affected by the mass transfer of a solute from a supersaturated liquid solution to a solid crystalline [16, 23, 24].

CONCLUSION: The complex nature of Urolithiasis necessitates a comprehensive understanding of the variables that influence the development of different phases of kidney stones. An intricate examination of kidney stones is essential to ascertain their etiology. The combined implementation of scanning electron microscopy, Fourier transform infrared spectroscopy, and X-ray diffraction is a valuable approach for identifying components present in extremely small proportions. We suggest the use of X-ray Rietveld analysis to further investigate the crystal structure and composition of kidney stones. This study has led to the identification of contributing factors for stone formation such as infectious nanobacteria, characteristic microstructural features associated with metabolic stones, and UTIs. Considering the involvement of bacterial infections in the formation of struvite stones, it is imperative to further investigate the association among UTI, multidrug-resistant bacteria (MDR), and stone formation and recurrence. It is reasonable to hypothesize that UTIs are a major cause of struvite stone formation within the Nagpur region. Hence, additional studies are necessary to confirm the role of bacterial infections in nidus formation.

ACKNOWLEDGEMENT: The authors are thankful to the department of Biochemistry for providing support for the study and to Dr. Prashant Shelke, Principal, Hislop College for facilities and encouragement.

Author Disclosure Statement: No competing financial interest exist.

Funding Information: Financial support from Union Grant Commission is gratefully acknowledged for granting research scholarship, (UGC-RGNF fellowship) to Apurva Wase.

REFERENCES:

1. Daudon M, Petay M, Vimont S, Deniset A, Tielens F, Haymann JP, Letavernier E, Frochot V and Bazin D: Urinary tract infection inducing stones: Some clinical and chemical data. Comptes Rendus Chimie 2022; 25: 315-334.
2. Rahman IA, Nusaly IF, Syahrir S, Nusaly H and Mansyur MA: Association between metabolic syndrome components and the risk of developing nephrolithiasis: A systematic review and bayesian meta-analysis. F1000 Research 2021; 10: 104.
3. Jung H, Andonian S, Assimos D, Averch T, Geavlete P, Kohjimoto Y, Neisius A, Philip J, Saita A, Shah H, Osther PJ. Urolithiasis: evaluation, dietary factors, and medical management: an update of the 2014 SIU-ICUD international consultation on stone disease. World Journal of Urology 2017; 35: 1331-40.
4. Bohndiek S, Cook E, Arvanitis C, Olivo A, Royle G, Clark A, Prydderch M, Turchetta R & Speller R: A CMOS active pixel sensor system for laboratory- based x-ray diffraction studies of biological tissue. Physics in Medicine & Biology 2008; 53(3): 655.
5. Ma RH, Luo XB, Li Q and Zhong HQ: The systematic classification of urinary stones combine-using FTIR and SEM-EDAX. International Journal of Surgery 2017; 41: 150-61.
6. Werner H, Bapat S, Schobesberger M, Segets D and Schwaminger SP: Calcium Oxalate Crystallization: Influence of pH, Energy Input, and Supersaturation Ratio on the Synthesis of Artificial Kidney Stones. ACS Omega 2021; 6: 26566–74.
7. Singh VK, Jaswal BS, Sharma J and Rai PK: Analysis of stones formed in the human gall bladder and kidney using advanced spectroscopic techniques. Biophysical Reviews 2020; 12: 647-68.
8. Chatterjee P, Chakraborty A and Mukherjee AK: Phase composition and morphological characterization of human kidney stones using IR spectroscopy, scanning electron

microscopy and X-ray Rietveld analysis. Spectrochimica Acta Part A: Molecular and Biomolecular Spectroscopy 2018; 200: 33–42.
9. Khan SR, Pearle MS, Robertson WG, Gambaro G, Canales BK, Doizi S, Traxer O, Tiselius HG. Kidney stones. Nature reviews Disease primers 2016; 2(1): 1-23.
10. Alemzadeh E, Farkhondeh T, Aschner M, Pourbagher-Shahri AM, Alemzadeh E, Salehinia H, Ranjbar Garmroodi BZ, Bideh M, Abedi F and Samarghandian S:Role of Nanobacteria in the Development of Nephrolithiasis: A Systematic Study. Current Nanoscience 2023; 19(2): 209-19.
11. Majidpour A, Rasouli S, Sardarabadi H, Noaparast M, Khedmatgozar M, Fathizadeh S, Ghooshchian M, Boustanshenas M and Sadat SA: The First Identification of Nanobacteria-Like Structures in Vascular Plaques of Atherosclerosis Patients in Iran. Archives of Clinical Infectious Diseases 2019; 14(4).
12. Kajander EO, Ciftcioglu N, Aho K and Garcia-Cuerpo E: Characteristics of nanobacteria and their possible role in stone formation. Urol Res 2003; 31: 47–54.
13. (Porikli) Durdağı S, Al- Jalawee AHH, Yalçin P, Bozkurt AS and Salcan S: Morphological characterization and phase determination of kidney stones using x-ray diffractometer and scanning electron microscopy. Chinese Journal of Physics 2023; 83: 379–88.
14. Cruz-May TN, Herrera A, Rodríguez-Hernández J, Basulto-Martínez M, Flores-Tapia JP and Quintana P: Structural and morphological characterization of kidney stones in patients from the Yucatan Maya population. Journal of Molecular Structure 2021; 1235: 130267.
15. Liu Y, Chen Y, Liao B, Luo D, Wang K, Li H & Zeng G: Epidemiology of urolithiasis in Asia. Asian Journal of Urology 2018; 5: 205–14.
16. Ferraro PM, Bargagli M, Trinchieri A and Gambaro G: Total, dietary, and supplemental vitamin c intake and risk of incident kidney stones. American Journal of Kidney Diseases 2016; 67: 400–7.
17. Stamatelou K and Goldfarb DS: Epidemiology of Kidney Stones. Healthcare 2023; 11: 424.
18. Prakash R, Arunachalam, Narayanasamy: Prevalence and socio-demographic status on kidney stone patients in Thanjavur district, Tamil Nadu, India. International Journal Of Community Medicine And Public Health 2019; 6: 1943.
19. Gujarathi DAP, Powar J, Palwe DS: A case-control study on risk factors for renal stones in a tribal area of Nashik, India. Journal of Cardiovascular Disease Research 2023: 2930-2944.
20. Pompilio A, Ranalli M, Piccirilli A, Perilli M, Vukovic D, Savic B, Krutova M, Drevinek P, Jonas D, Fiscarelli E, Tuccio Guarna Assanti V, Tavío M, Artiles F & Di Bonaventura G: Biofilm formation among *Stenotrophomonas maltophilia* isolates has clinical relevance: the anselm prospective multicenter study. Microorganisms 2020; 9: 49.
21. Letavernier E, Bazin D and Daudon M: Description of Stone Morphology and Crystalluria Improve Diagnosis and Care of Kidney Stone Formers. Healthcare 2022; 11: 2.
22. Manzoor MA, Agrawal AK, Singh B, Mujeeburahiman M, Rekha PD. Morphological characteristics and microstructure of kidney stones using synchrotron radiation μCT reveal the mechanism of crystal growth and aggregation in mixed stones. PloS one 2019; 14(3).
23. Izatulina AR, Gurzhiy VV, Krzhizhanovskaya MG, Kuz'mina MA, Leoni M and Frank-Kamenetskaya OV: Hydrated calcium oxalates: crystal structures, thermal stability, and phase evolution. Crystal Growth & Design 2018; 18: 5465–78.
24. Wallace B, Chmiel JKF, Bjazevic J, Burton J, Goldberg H, & Razvi H: The Role of Urinary Modulators in the Development of Infectious Kidney Stones. Journal of Endourology 2023; 37: 358–66.

How to cite this article:
Wase AS, Sarkar S and Pise M: Characterizing microstructures and crystallographic phases in kidney stones from the Nagpur region, Maharashtra. Int J Pharm Sci & Res 2024; 15(5): 1433-40. doi: 10.13040/IJPSR.0975-8232.15(5).1433-40.